FEBS Letters 588 (2014) 3213–3217

journal homepage: www.FEBSLetters.org

Catalytic role of the calcium ion in GH97 inverting glycoside hydrolase

Masayuki Okuyama [a,*,1], Takuya Yoshida [a,1], Hironori Hondoh [a,b], Haruhide Mori [a], Min Yao [c], Atsuo Kimura [a]

[a] Research Faculty of Agriculture, Hokkaido University, Sapporo, Hokkaido 060-8589, Japan
[b] Graduate School of Biosphere Science, Hiroshima University, Higashihiroshima, Hiroshima 739-8528, Japan
[c] Faculty of Advanced Life Science, Hokkaido University, Sapporo, Hokkaido 060-0810, Japan

ARTICLE INFO

Article history:
Received 12 June 2014
Revised 30 June 2014
Accepted 2 July 2014
Available online 10 July 2014

Edited by Stuart Ferguson

Keywords:
Glycoside hydrolase family 97
Calcium ion dependent glycosidase
Structural analysis
Kinetic analysis

ABSTRACT

The role of calcium ion in the active site of the inverting glycoside hydrolase family 97 enzyme, *Bt*GH97a, was investigated through structural and kinetic studies. The calcium ion was likely directly involved in the catalytic reaction. The pH dependence of k_{cat}/K_m values in the presence or absence of calcium ion indicated that the calcium ion lowered the pK_a of the base catalyst. The significant decreases in k_{cat}/K_m for hydrolysis of substrates with basic leaving groups in the absence of calcium ion confirmed that the calcium ion facilitated the leaving group departure.

1. Introduction

Several glycoside hydrolases require the participation of a metal ion for catalysis. For instance, *exo*-mannosidases belonging to glycoside hydrolase families (GH) 38, 47, and 92 require a divalent metal ion, such as zinc or calcium. The metal ion bridges the C2 and C3 oxygen atoms and is associated with the stabilization of the transition state [1]. GH4 glycoside hydrolases which employ an unique redox-elimination mechanism to cleave the glycosidic linkage require a divalent metal ion for catalysis [2]. The divalent ion helps to stabilize the enediolate intermediate, which arises during redox-elimination. GH2 β-galactosidase uses a magnesium ion for catalysis. The magnesium ion makes direct contact with the acid/base catalyst and thus functions in tuning the pK_a of the acid/base catalyst [3,4].

GH97 is an unique family that contains an inverting α-glucoside hydrolase (*Bt*GH97a) and a retaining α-galactoside hydrolase (*Bt*GH97b) [5–7]. Both enzymes contain one calcium ion in the active site which plays an important role in the catalysis of both enzymes, likely orienting functional residues and/or acting as a Lewis acid. Indeed, incubation with EDTA causes substantial reduction of their catalytic activity [5,6]. The calcium ion in the ligand-free inverting *Bt*GH97a is coordinated by four glutamate residues (Glu194, Glu508, Glu526, and Glu532) and three water molecules (Fig. 1A). Three water molecules are replaced by the O2 of the valienamine unit, the O3 and N4B of the 4-amino-4,6-dideoxy α-D-glucose unit in the acarbose-complex form (Fig. 1B). The interaction with N4B is of interest because N4B is the pseudo-scissile bond atom in acarbose and the calcium ion seems to be directly involved in catalysis. Among the amino-acid residues coordinated with the calcium ion, Glu508 and Glu532 are closely involved with the catalytic reaction. The inverting glycoside hydrolase possesses two functional groups, which act as catalytic acid and base, in the active site. The catalytic acid transfers the proton to the oxygen atom in the scissile glycosidic linkage and promotes the departure of the substrate leaving group. The catalytic base activates a catalytic water molecule to abstract the proton, with the water molecule attacking on the anomeric carbon of the substrate. The carboxy group of Glu532 is then poised to act as the catalytic acid. The side chain of Glu508 interacts with the water molecule in position for an in-line attack at the anomeric center together with the carboxy group of Glu439, both functioning as catalytic bases in the

Abbreviations: BSA, bovine serum albumin; 2C4NPG, 2-chloro-4-nitrophenyl α-D-glucopyranoside; 4C2NPG, 4-chloro-2-nitrophenyl α-D-glucopyranoside; 2,4DNPG, 2,4-dinitrophenyl α-D-glucopyranoside; 3,4DNPG, 3,4-dinitrophenyl α-D-glucopyranoside; EDTA, ethylenediamine-*N,N,N′,N′*-tetraacetic acid; GH, glycoside hydrolase family; MNPG, *m*-nitrophenyl α-D-glucopyranoside; PNPG, *p*-nitrophenyl α-D-glucopyranoside

* Corresponding author. Address: Division of Applied Bioscience, Research Faculty of Agriculture, Hokkaido University, Kita-9, Nishi-9, Kita-ku, Sapporo, Hokkaido 060-8589, Japan. Fax: +81 11 706 2808.
E-mail address: okuyama@abs.agr.hokudai.ac.jp (M. Okuyama).
[1] First two authors contributed equally to this work.

http://dx.doi.org/10.1016/j.febslet.2014.07.002
0014-5793/

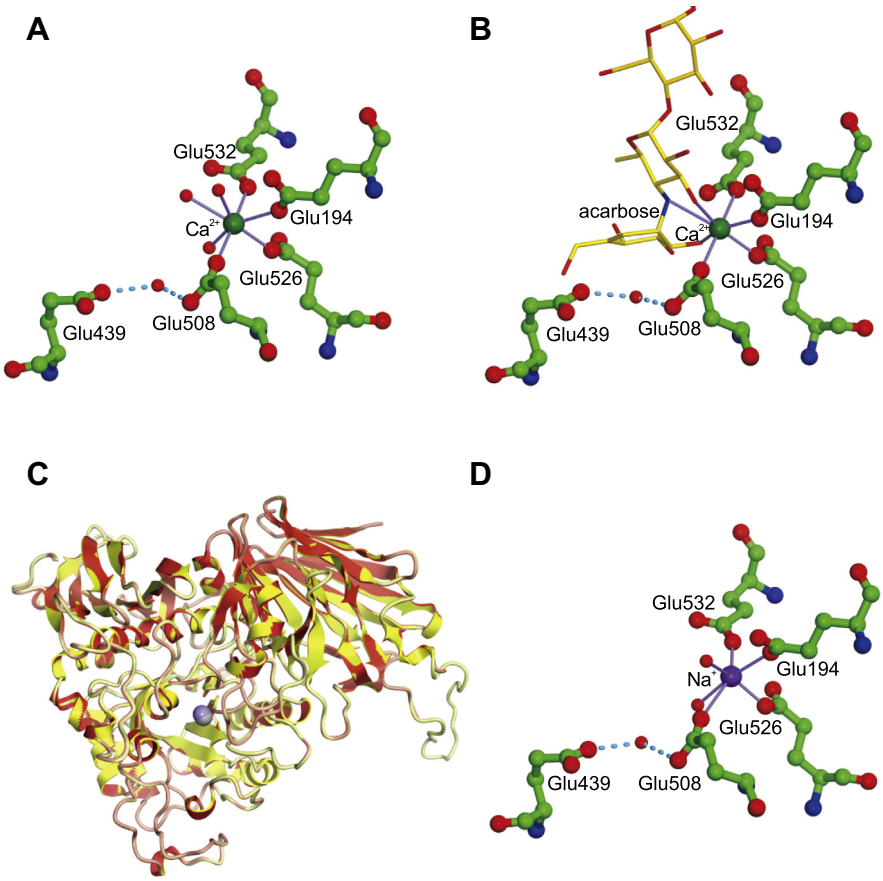

Fig. 1. Structural comparison of *Bt*GH97a and EDTA-treated *Bt*GH97a. The calcium ion binding sites, native *Bt*GH97a (A; PDB ID, 2D73), and acarbose-complex *Bt*GH97a (B; PDB ID, 2ZQ0). (C) Overall structure of the EDTA-treated *Bt*GH97a (red) with native *Bt*GH97a (yellow). (D) The sodium ion binding in the EDTA-treated *Bt*GH97a. Figures were created using CueMol 2 (http://cuemol.sourceforge.jp/).

inverting mechanism. The retaining α-galactosidase, *Bt*GH97b, contains a calcium ion at the same position as *Bt*GH97a [7]. It has three equivalent carboxy groups, corresponding to Glu194, Glu526 and Glu532, and four water molecules, which are associated with the calcium binding. Since the enzyme does not have a residue equivalent to Glu508, one water molecule of the four is located at the same position as the carboxy group of Glu508, and makes a hydrogen bond to the residue functioning as the nucleophile catalyst in the retaining mechanism.

The purpose of this study was to elucidate the role of the calcium ion in the catalysis of the inverting *Bt*GH97a using kinetic studies and analysis of the crystal structure of EDTA-treated *Bt*GH97a. These studies revealed that the calcium ion participates in the catalysis differently from what was previously observed for other GHs, as it stabilizes the deprotonated state of the base catalyst and assists in the departure of the substrate leaving group.

2. Materials and methods

2.1. Materials

p-Nitrophenyl α-D-glucopyranoside (PNPG) was purchased from Nacalai Tesque (Kyoto, Japan). Aryl glucosides, 2,4-dinitrophenyl, 2-chloro-4-nitrophenyl, and 4-chloro-2-nitrophenyl α-D-glucopyranosides (2,4DNPG, 2C4NPG, and 4C2NPG) were synthesized according to a published procedure [8]. Other aryl glucosides, 3,4-dinitrophenyl and *m*-nitrophenyl α-D-glucopyranosides (3,4DNPG and MNPG, respectively), were synthesized from 1,2,3,4,6-penta-*O*-acetyl-D-glucopyranose and the corresponding phenol derivative with trifluoromethane sulfonic acid as a catalyst. Under a nitrogen atmosphere, trifluoromethane sulfonic acid (5.5 mmol) was added to a mixture of 1,2,3,4,6-penta-*O*-acetyl-D-glucopyranose (5.5 mmol) and the desired phenol (11 mmol) in 10 mL of dichloromethane. The mixture was stirred for 3 h at room temperature, and then dry pyridine (4 mL) and acetic anhydride (0.95 mL) were added and stirred for 1 h at room temperature. Sodium acetate trihydrate (1.8 g) was added to the mixture and it was stirred vigorously for several minutes. Saturated $NaHCO_3$ solution was added and the organic layer was extracted with dichloromethane, washed with ice-cold water, and dried over Na_2SO_4. Pyridine was removed by co-evaporation with toluene and the product was purified by column chromatography, performed on 40–50 μm silica gel (2:1 hexane/ethyl acetate for *m*-nitrophenyl 2,3,4,6-tetra-*O*-acetyl-α-D-glucopyranoside, 3:2 hexane/ethyl acetate for 3,4-dinitrophenyl 2,3,4,6-tetra-*O*-acetyl-α-D-glucopyranoside). The ^1H NMR spectra of all aryl per-*O*-acetyl-glucosides were identical to published data [8,9]. Deacetylation of 2,4-dinitrophenyl, 2-chloro-4-nitrophenyl, and 3,4-dinitrophenyl 2,3,4,6-tetra-*O*-acetyl-α-D-glucopyranosides were performed by the acetyl chloride method [8] and 4-chloro-2-nitrophenyl and *m*-nitrophenyl 2,3,4,6-tetra-*O*-acetyl-α-D-glucopyranosides were deacetylated with sodium methoxide in dry methanol.

2.2. Enzyme purification

The genes encoding the wild-type *Bt*GH97a and the E532Q mutant were amplified from previously constructed plasmid DNAs [6] by PCR. Each resultant fragment was ligated into the pET23d

plasmid (Novagen, Billerica, MA). Plasmid DNAs were designed to include a hexahistidine tag at the C-terminal of the recombinant protein. *Escherichia coli* BL21 (DE3) RIL (Stratagene, Wilmington, DE) was used for recombinant protein production. Recombinant proteins were expressed in LB with 100 μg/mL of ampicillin at 37 °C overnight without addition of IPTG. The recombinant proteins were purified with Ni-Sepharose FF (GE Healthcare, Buckinghamshire, England) affinity chromatography using 0.1 M Mes-NaOH (pH 7.0)/0.3 M NaCl as a basal buffer. The protein fractions, eluted by increasing the imidazole concentration, were subjected to Sephadex G-25 column chromatography equilibrated with 0.1 M Mes-NaOH (pH 7.0 containing 0.1 M NaCl and 0.2 mg/mL sodium azide). The purified protein fractions were concentrated using a Centriprep YM-50 (Millipore, Billerica, MA). The protein for crystallization was further purified by gel filtration using Sephacryl S-200 (GE Healthcare) equilibrated with 0.1 M Mes-NaOH (pH 7.0) containing 100 mM NaCl, 10 mM ethylenediamine-*N,N,N′,N′*-tetraacetic acid, disodium salt (EDTA·2Na) and 0.2 mg/mL sodium azide.

2.3. Crystallization, data collection, structure determination, and refinement

The crystal of the EDTA-treated *Bt*GH97a was grown at 25 °C by the hanging-drop vapor diffusion method using a reservoir solution containing 12% (w/v) polyethylene glycol 6000 and 0.1 mM imidazole–HCl (pH 7.8). In addition, 4% (w/v) 2-propanol was added to the droplet of the protein. A data set was collected at 100 K on an R-AXIS IV imaging plate diffractometer using an in-house CuK_α (1.54 Å) source (Rigaku MicroMax 007, Tokyo, Japan). For data collection, the crystal was soaked in a reservoir solution supplemented with 25% (v/v) 2-methyl-2,4-pentanediol. Diffraction data sets were processed using the programs Mosflm and SCALA in the CCP4 suite [10]. The structure was determined at a resolution of 2.0 Å by the molecular replacement method using the structure of the native *Bt*GH97a as a search model with the program AMoRe [11] in the CCP4 suite. The model building and manual mode corrections were carried out using the program CNS [12]. The statistics of data collection and refinement are summarized in Supplemental Table 1. Coordinates and structure factors have been deposited in the Protein Data Bank with the accession number 3WFA.

2.4. pH-dependence studies

The pH dependence of k_{cat}/K_m for hydrolysis of PNPG by wild-type enzyme was calculated by dividing the first-order rate constants by the enzyme concentration. The rate constants were measured at a sufficiently low substrate concentration ([S] = 10 μM ≪ K_m) using the following buffers: 50 mM maleic acid–NaOH (pH 5.0–7.0), 50 mM Hepes–NaOH (pH 7.0–8.5), and 50 mM glycine–NaOH (pH 8.5–9.5). All buffers contained 0.01 mg/mL BSA and 2 mM EDTA·2Na. For analysis of the pH-dependence of k_{cat}/K_m in the presence of calcium ion, 10 mM $CaCl_2$ was added to each buffer. The enzyme concentrations used were 2.3–23 nM for measurements without calcium ion, and 0.9–4.6 nM for measurements with calcium ion. The reaction mixture was incubated at 27 °C, and at 5–40 min an aliquot of the mixture was removed and mixed with a double volume of 1 M sodium carbonate/50 mM EDTA. The amount of *p*-nitrophenol released was measured by absorption at 400 nm in a 1-cm cuvette, considering a molar extinction coefficient of 5560 M^{-1} cm^{-1}. The first-order rate curves generated at each pH were fit to the first-order rate equation ($\ln([A]_t/[A]_0) = -kt$) to determine the rate constant k, which is comparable to k_{cat}/K_m. The rate constant obtained at each pH were fitted to a theoretical bell-shaped ionization curve [k_{cat}/K_m = $\{\text{limit} \times 10^{(pH-pKe1)}\}/\{10^{(2\times pH-pKe1-pKe2)} + 10^{(pH-pKe1)} + 1\}$] using the computer program GraFit 7 (Erithacus Software Ltd.).

The kinetic constants for E532Q for the hydrolysis of PNPG at various pH values were calculated by fitting to the Michaelis–Menten equation by non-linear regression. The initial velocities of hydrolysis of PNPG at 27 °C were measured at six substrate concentrations (0.1–2.0 mM) in the same buffers used for wild-type enzyme but with a $CaCl_2$ concentration of 80 mM instead of 10 mM. The enzyme concentrations used were 0.51–1.5 μM for measurements without calcium ion and 15 nM for measurements with calcium ion, respectively. The velocities were calculated by subtracting the rate of the spontaneous degradation from that of the observed hydrolysis. The k_{cat}/K_m value determined at each pH was fit with a function describing a single ionization process [k_{cat}/K_m = limit/$\{10^{(pKe1-pH)} + 1\}$].

2.5. Kinetic parameters of E532Q for aryl α-glucosides

Michaelis–Menten parameters for aryl glucosides (2,4DNPG, 3,4DNPG, 2C4NPG, and 4C2NPG) were measured by monitoring the release of phenol derivatives at a wavelength of 405 nm using a MULTISKAN ASCENT plate reader (Thermo Scientific, Waltham, MA). All reactions were performed at 27 °C, pH 9.5, in a 96-well microplate. Each reaction well contained substrate and 50 mM glycine-NaOH buffer, pH 9.5 in a total volume of 160 μL. For measurement of the hydrolytic rate in the presence of calcium ion, a buffer containing 100 mM $CaCl_2$ was used. The substrate concentration range employed was 0.1–2.0 mM. After the microplate was preincubated at 27 °C, 40 μL of diluted E532Q (76–760 nM in 50 mM glycine–NaOH, pH 9.5, containing 0.5 mg/mL BSA and 10 mM EDTA·2Na) was added. The molar extinction coefficient, ε, of each phenol derivative at pH 9.5 was determined by measuring the absorbance of various concentrations of the phenol derivative. For determination of the kinetic constants for PNPG and MNPG, the reaction was performed using a test tube and the amount of *p*- or *m*-nitrophenol released was measured by absorption at 400 nm in a 1-cm cuvette. Kinetic parameters were calculated by fitting the data to the Michaelis–Menten equation. Logarithms of the obtained k_{cat}/K_m values were linearly fit with leaving group pK_a values.

3. Results and discussion

3.1. Three-dimensional structure of EDTA-treated BtGH97a

The crystal structure of *Bt*GH97a treated with 2 mM EDTA was determined at a resolution of 2.0 Å with the molecular replacement method using the structure of a native *Bt*GH97a (PDB ID 2d73) as a search model. The overall structure was nearly identical to that of the native *Bt*GH97a with a root mean square deviation of 0.17 Å (Fig. 1C). A sodium ion was found at the active site in place of the calcium ion (Fig. 1D). The sodium ion was coordinated by four glutamate residues (Glu194, Glu508, Glu526, and Glu532) and two water molecules. These residues are equivalent to the residues that coordinate the calcium ion in the native *Bt*GH97a. Compared with the native *Bt*GH97a, EDTA-treated *Bt*GH97a had one less ligand water molecule (Fig. 1A and D). The lost water molecule corresponded to the water molecule that was replaced by the pseudo-scissile bond atom in the previous acarbose-complex structure (Fig. 1B and D) [6]. Accordingly, EDTA-treated *Bt*GH97a appears to lose the interaction with the scissile bond of the substrate through the metal ion.

3.2. Effect of calcium ion on pH-dependence

The pH-dependency of k_{cat}/K_m for hydrolysis of PNPG by the EDTA-treated *Bt*GH97a in the presence of 10 mM $CaCl_2$ or in the

absence of calcium ion was evaluated. k_{cat}/K_m was estimated by the first-order rate constants at sufficiently low substrate concentrations. The approximated k_{cat}/K_m values were fitted to a bell-shaped ionization curve (Fig. 2A). The maximum approximate k_{cat}/K_m value in the presence of calcium ion was observed at pH 6.5 (1430 s^{-1} mM^{-1}) and with calculated pK_{e1} of 4.7 and a pK_{e2} of 7.8 (where pK_{e1} and pK_{e2} represent the pK_e values of the acidic limb and the basic limb, respectively). In the absence of calcium ion, the optimum pH shifted to pH 8.2 and the maximum value was reduced seven times from that in the presence of calcium ion (206 s^{-1} mM^{-1}). The absence of calcium ion shifted pK_{e1} and pK_{e2} 3.0 and 0.7 pH units higher, respectively (pK_{e1} = 7.7 and pK_{e2} = 8.5). pK_{e1} and pK_{e2} reflect the ionization states of the catalytic base and acid in the inverting mechanism, respectively, and the presence of the calcium ion was found to significantly lower the ionization state of the catalytic base while only slightly affecting that of the catalytic acid.

*Bt*GH97a has two glutamate residues that are closely involved in the base catalysis, Glu439 and Glu508. It is difficult to distinguish which is the actual catalytic base based on the tertiary structure since both residues make interactions with the catalytic water (Fig. 1B). Glu508 makes contact with the calcium ion, and its ionization state is likely to reflect pK_{e1}. A study by Wang et al. using a quantum mechanical/molecular mechanical method supports the notion that the carboxy group of Glu508 is likely the catalytic base [13]. Stabilization of the dissociation state of the catalytic base would help it to abstract a proton from the catalytic water and enhance its nucleophilicity to catalyze the inverting hydrolysis of the substrate. The positive charge from the sodium ion found in the active site of the EDTA-treated *Bt*GH97a might be insufficient to maintain the deprotonated state of the carboxy group of Glu508.

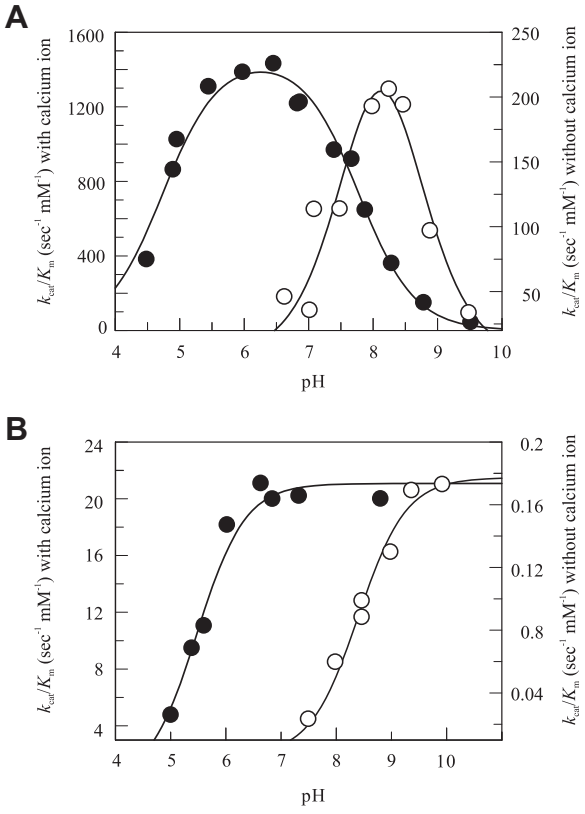

Fig. 2. Dependence of the kinetic constant k_{cat}/K_m on pH for the hydrolysis of PNPG in the presence (●) or absence (○) of calcium ion. (A) Wild-type *Bt*GH97a, (B) E532Q *Bt*GH97a.

The involvement of a calcium ion to assist the catalytic base in *Bt*GH97a would be an unique feature among glycoside hydrolases. Most inverting glycoside hydrolases bear the machinery for supporting the function of a catalytic base, generally through the involvement of amino acid residues surrounding the catalytic base. For instance, the function of the catalytic base of GH15 *Aspergillus awamori* glucoamylase, an α → β inverting glycoside hydrolase, is maintained by interactions with the side chains of Tyr48 and Ser411 [14,15].

3.3. Effect of calcium ion on the catalytic acid

The pH-dependences of k_{cat}/K_m for hydrolysis of PNPG by E532Q in the presence of 80 mM $CaCl_2$ or in the absence of calcium ion were measured. The basic limb of the pH-profile disappeared and k_{cat}/K_m values were fitted to a single ionization curve (Fig. 2B). The distinct pH-dependence of E532Q indicated that Glu532 acts as a Brønsted acid catalyst in the inverting mechanism. The presence of calcium ion shifted pK_{e1} approximately 2.9 pH units lower (pK_{e1} = 5.5 and pK_{e1} = 8.4 in the presence and the absence of calcium ion, respectively). The shift in the pK_{e1} to the acidic region in the presence of calcium ion may be explained by examining the role of the calcium ion in the wild-type enzyme.

The previous structural analysis showed that the calcium ion seemed to be directly involved in catalysis since the calcium ion was coordinated by the pseudo-scissile atom, N4B of acarbose (Fig. 1B) [6]. To further examine this, the kinetic parameters of E532Q for the hydrolysis of a series of aryl α-glucosides with a range of differing phenol leaving group abilities were measured in the presence of 80 mM $CaCl_2$ or in the absence of calcium ion (Supplementary Table 2). E532Q was used to eliminate the effect of Brønsted acid catalysis. The K_m value for MNPG in the absence of calcium ion was so large that only a k_{cat}/K_m value was estimated from the rate constant, which was determined at the sufficiently low substrate concentration ([S] = 4 mM). The logarithms of k_{cat}/K_m values were plotted against the pK_as of the leaving groups (Fig. 3). Linear relationships were found between pK_a and log (k_{cat}/K_m) in the presence and absence of calcium ion. Slopes were −1.0 without calcium ion and −0.029 with calcium ion, respectively. The k_{cat}/K_m values in the absence of calcium ion were more sensitive to the changes of the pK_a of the leaving groups than those in the presence of calcium ion. The significance decreases in k_{cat}/K_m for the hydrolysis of the substrates with basic leaving groups in the absence of calcium ion were consistent with the conclusion that the calcium ion participates in acid catalysis of the leaving group departure because cleavage of basic leaving groups requires the participation of an acid catalyst. The difference in the slopes in

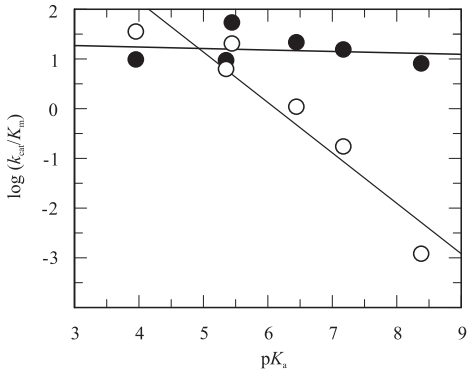

Fig. 3. Dependence of log (k_{cat}/K_m) on pK_a for the E532Q *Bt*GH97a-catalyzed hydrolyses of aryl α-glucosides in the presence (●) or absence (○) of calcium ion.

the presence of calcium ion versus its absence implies that either a change in a rate-limiting step occurs or the calcium ion almost completely neutralizes negative charge developing on the phenolate oxygen in E532Q. The former interpretation is quite unlikely in view of the single displacement of the inverting mechanism. The rate-limiting step would involve breakage of the glycosidic linkage. Therefore, little negative charge would be present on the glycosidic oxygen at the transition state in the case of E532Q. However, this would not hold exactly in the wild-type enzyme.

In wild-type *Bt*GH97a, the calcium ion is not the predominant acid catalyst for the cleavage of the glycosidic linkage, and instead the carboxy group of Glu532 fulfills that role. This is because inactivation of the enzyme by the mutation of Glu532 is more effective at eliminating enzyme activity than the removal of the calcium ion. The pH-dependence of the wild-type enzyme in the absence of calcium ion exhibits a bell-shape curve (Fig. 2A), while the pH dependence of k_{cat}/K_m for the acid catalyst mutant, E532Q, in the presence of calcium ion shows a single ionization curve (Fig. 2B). In addition, if direct electrophilic attack by the calcium ion on the glycosidic oxygen occurred, the cleavage of the glycosidic bond would lead to the formation of a Ca–OR complex and the calcium ion would shift position. Wang et al. reported, however, that the calcium ion theoretically maintains a similar coordination with the glycosidic oxygen during the catalytic reaction [13]. Therefore, we concluded that the calcium ion functions in a secondary role, decreasing the basicity and facilitating the departure of the leaving group, while the predominant acid catalyst role is fulfilled by Glu532. A theoretical study also suggested that the catalytic reaction of *Bt*GH97a is initiated by nucleophile attack of the water followed by proton transfer from the acid catalyst [13]. It is possible that the calcium develops an electron-poor anomeric carbon through its interaction to the glycosidic oxygen and facilitates the nucleophilic attack.

In conclusion, this study suggests that the role of the calcium ion in the catalytic reaction of GH97 inverting enzyme is to function as a stabilizer of the base catalyst and to facilitate the departure of the substrate leaving group. To the best of our knowledge, these roles have not been previously described for calcium in the catalytic reaction of GHs.

Acknowledgments

We thank Dr. Eri Fukushi of the GC–MS & NMR Laboratory, Faculty of Agriculture, Hokkaido University for MS and NMR analyses, and Mr. Tomohiro Hirose of the Instrumental Analysis Division, the Equipment Management Center, Creative Research Institution, Hokkaido University for amino acid analysis.

Appendix A. Supplementary data

Supplementary data associated with this article can be found, in the online version, at http://dx.doi.org/10.1016/j.febslet.2014.07.002.

References

[1] Zhu, Y., Suits, M.D., Thompson, A.J., Chavan, S., Dinev, Z., Dumon, C., Smith, N., Moremen, K.W., Xiang, Y., Siriwardena, A., Williams, S.J., Gilbert, H.J. and Davies, G.J. (2010) Mechanistic insights into a Ca^{2+}-dependent family of α-mannosidases in a human gut symbiont. Nat. Chem. Biol. 6, 125–132.

[2] Rajan, S.S., Yang, X., Collart, F., Yip, V.L., Withers, S.G., Varrot, A., Thompson, J., Davies, G.J. and Anderson, W.F. (2004) Novel catalytic mechanism of glycoside hydrolysis based on the structure of an NAD^+/Mn^{2+}-dependent phospho-α-glucosidase from *Bacillus subtilis*. Structure 12, 1619–1629.

[3] Richard, J.P., Huber, R.E., Lin, S., Heo, C. and Amyes, T.L. (1996) Structure-reactivity relationships for β-galactosidase (*Escherichia coli*, lac Z). 3. Evidence that Glu-461 participates in Brønsted acid-base catalysis of β-D-galactopyranosyl group transfer. Biochemistry 35, 12377–12386.

[4] Juers, D.H., Heightman, T.D., Vasella, A., McCarter, J.D., Mackenzie, L., Withers, S.G. and Matthews, B.W. (2001) A structural view of the action of *Escherichia coli* (lacZ) β-galactosidase. Biochemistry 40, 14781–14794.

[5] Gloster, T., Turkenburg, J., Potts, J., Henrissat, B. and Davies, G. (2008) Divergence of catalytic mechanism within a glycosidase family provides insight into evolution of carbohydrate metabolism by human gut flora. Chem. Biol. 15, 1058–1067.

[6] Kitamura, M., Okuyama, M., Tanzawa, F., Mori, H., Kitago, Y., Watanabe, N., Kimura, A., Tanaka, I. and Yao, M. (2008) Structural and functional analysis of a glycoside hydrolase family 97 enzyme from Bacteroides thetaiotaomicron. J. Biol. Chem. 283, 36328–36337.

[7] Okuyama, M., Kitamura, M., Hondoh, H., Kang, M., Mori, H., Kimura, A., Tanaka, I. and Yao, M. (2009) Catalytic mechanism of retaining α-galactosidase belonging to glycoside hydrolase family 97. J. Mol. Biol. 392, 1232–1241.

[8] Chen, H.M. and Withers, S.G. (2007) Facile synthesis of 2,4-dinitrophenyl α-D-glycopyranosides as chromogenic substrates for α-glycosidases. Chem. Bio. Chem. 8, 719–722.

[9] Lee, S.S., Yu, S. and Withers, S.G. (2003) Detailed dissection of a new mechanism for glycoside cleavage: α-1,4-glucan lyase. Biochemistry 42, 13081–13090.

[10] Bailey, S. (1994) The CCP4 Suite – programs for protein crystallography. Acta Crystallogr. Sect. D Biol. Crystallogr. 50, 760–763.

[11] Navaza, J. (1994) AMORE – an automated package for molecular replacement. Acta Crystallogr. Sect. A 50, 157–163.

[12] Brunger, A., Adams, P., Clore, G., DeLano, W., Gros, P., Grosse-Kunstleve, R., Jiang, J., Kuszewski, J., Nilges, M., Pannu, N., Read, R., Rice, L., Simonson, T. and Warren, G. (1998) Crystallography & NMR system: a new software suite for macromolecular structure determination. Acta Crystallogr. Sect. D Biol. Crystallogr. 54, 905–921.

[13] Wang, J., Sheng, X., Zhao, Y., Liu, Y. and Liu, C. (2012) QM/MM investigation on the catalytic mechanism of Bacteroides thetaiotaomicron α-glucosidase BtGH97a. Biochim. Biophys. Acta 1824, 750–758.

[14] Frandsen, T.P., Dupont, C., Lehmbeck, J., Stoffer, B., Sierks, M.R., Honzatko, R.B. and Svensson, B. (1994) Site-directed mutagenesis of the catalytic base glutamic acid 400 in glucoamylase from Aspergillus niger and of tyrosine 48 and glutamine 401, both hydrogen-bonded to the γ-carboxylate group of glutamic acid 400. Biochemistry 33, 13808–13816.

[15] Fang, T.Y. and Ford, C. (1998) Protein engineering of Aspergillus awamori glucoamylase to increase its pH optimum. Protein Eng. 11, 383–388.